PROSTHETIC ARACHNOID GRANULATIONS USING 3D PRINTING TECHNOLOGY

Tzu-Li Liu,[1,2], Sulmaz Zahedi[3,5], R. Justin Garling[3], Francis Kralick[6], Carolyn A. Harris[3,4], and Mark Ming-Cheng Cheng[2,4]

[1]Electronic Engineering, Chang-Gung University, Taiwan,
[2]Electrical and Computer Engineering, [3]Department of Neurosurgery,
[4]Biomedical Engineering Wayne State University, Detroit MI,
[5]University of Toronto Institute of Biomaterials and Biomedical Engineering,
[6]Shore Physicians Group

ABSTRACT

Hydrocephalus, a disorder of excess cerebrospinal fluid, affects roughly 1 in 500 live births per year. Communicating, or extra-ventricular hydrocephalus, is a subset of the disorder that is, in part, a result of arachnoid granulation dysfunction. Arachnoid granulations are innate one-way valves that allow for pressure dependent absorption of cerebrospinal fluid from the subarachnoid space into the venous blood flow of the superior sagittal sinus. This study investigates a bead-based microfluidic diode as a self-regulated shunt valve for mimicking the physiological functions of arachnoid granulations. The proposed device has been fabricated using assembly of several parts manufactured by 3D printing (stereolithography). The additive manufacturing allows layer-by-layer deposition of soft polymer with high precision. The performance of bead-based arachnoid granulations has been preliminarily tested, including penetration into biological tissues and benchtop flow tests.

INTRODUCTION

Hydrocephalus is a result of dilatation of the cerebral ventricular system and can be obstructive (ventricular hydrocephalus) or non-obstructive (extra-ventricular hydrocephalus). Dysfunction of arachnoid granulations, one of the key sites of pressure dependent cerebrospinal fluid (CSF) absorption, is believed to be a primary cause of extra-ventricular hydrocephalus [1]. The standard of care for symptomatic hydrocephalus is the surgical insertion of a shunt system, which most commonly diverts CSF from the ventricle to the peritoneum, atrium, or pleura (Fig 1a). After just ten years, 85% of shunt systems fail, secondary to mechanical failure, shunt infection, or overdrainage, requiring subsequent revision [2]. While several groups have developed MEMS-based shunt systems using membrane structures [4-6], challenges remain, including mechanical failure, biocompatibility and flow control under low Reynolds number. Recently, microfabricated arachnoid granulations (MAG) have been suggested as an impressive alternative to shunting (Fig 1b) [4]. However, micro-fabrication processes for prototyping are expensive, time consuming, and require trained expertise. To overcome these challenges, particularly in the prototyping and testing phases, we augment the ideas presented by the MAG group with a simple yet novel 3D printing approach to form the prosthetic arachnoid granulations (bead-based MAG) consisting of (1) high precision 3D microchannels with in-line suspended microbeads to passively regulate flow, (2) an array of microneedles which form CSF flow channels, and (3) closed, biodegradable, microneedle tips to improve device implantation. Although there is literature on bead-based valves [6], to the best of our knowledge, this is the first report on the 3D-printed autonomous self-regulation valve system, which may be useful to accomplish many biological functions.

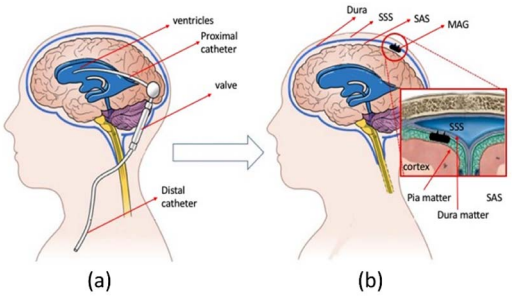

Fig 1. *Hydrocephalic patient with (a) ventriculoperitoneal shunt with truncated distal catheter and (b) the proposed arachnoid granulation prosthetic.*

EXPERIMENTS

A. The Working Principle of Devices: The proposed prosthetic arachnoid granulations will be implanted with their microneedles penetrating through the dura mater, allowing CSF to drain from the subarachnoid space (SAS) to the superior sagittal sinus (SSS). To implement the bead-based MAG, cylindrical microchannels were designed with stopping structures fabricated at the two ends, where a suspended microbead moves to regulate the flow depending on flow polarity. As shown in Fig 2(a), when the pressure in SAS (P_2) is greater than that in SSS (P_1), the microbead moves to the end with

a larger cross-section, allowing for pressure dependent CSF flow through the device. Conversely, when $P_1 > P_2$, the microbead moves to the end with a smaller cross-section, occluding the flow of CSF.

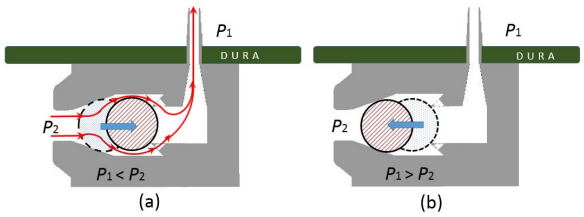

Fig 2. *Fluid flow through valve using a suspended microbead (a) SAS (P_2)>SSS Forward flow (P_1) (b) SSS (P_1) >SAS (P_2) Reverse flow*

B. 3D Printing: Due to the complex 3D structures in the design, stereolithography was used to create the prototype in a layer-by-layer fashion using photopolymerization. A commercial 3D printing system "PROJET 1200" with 50µm resolution was used. Photosensitive resin (VisiJet FTX Clear) was used, which contained 50% triethylene glycol diacrylate, 20% isobornyl methacrylate, 2% phenylbis (2,4,6-trimethyl benzoyl)- phosphine oxide. In the process, digital light processing (DLP) controlled and projected illumination of ultraviolet (UV) along the bottom of the resin to solidify the resin and form a single layer of the 3D object. The process was repeated until completion of the desired structure. After which, the object was immersed into 70% isopropyl alcohol (IPA) in a sonication bath for 5min to remove any residue on the surfaces, and was dried with di-nitrogen gas (N_2). Finally, the object was cured in a UV oven for 30 minutes to ensure smooth surface properties.

C. The Coating Process of Biodegradable Polymer: In order to ease penetration through the dura mater during future in vivo implantation, a two-step process was developed to add sharp sugar needles on the surfaces of the hollow microneedles. The first coating process occurred at a temperature T_1 (275C), where caramelizing sugar had a low viscosity and low surface tension. The microneedles were immersed tip first into the caramelized sugar coating mixture, and pulled out at a speed of V_1=5~10 mm/s. The second coating was completed at a temperature T_2 (175C). In the second coat, microneedles were immersed tip first, and pulled out of the coating mixture at a speed of V_2= 800 um/s.

D. Mechanical Tests: The mechanical performance of sugar coated hollow microneedles was evaluated by penetrating them into porcine skin. Prior to testing, the microneedles were stained with Trypan blue color dye. The speed of insertion was controlled V_p= 15-20 cm/s. All the tests were conducted at room temperature.

E. Benchtop Flow Tests: The bead-based shunt valve was evaluated using the flow setup shown in Fig. 6. The valves were printed in a customized external cylinder, to allow for secure connections into the Luer fittings for testing purposes. The cylinder geometry allows the matching of the valve (on two sides) and Luer connector (Cole-Parmer ID 1/8''), while maintaining the physiological internal measurements of the valve. Silicone tubing with a similar diameter was connected to the exterior of the Luer fitting. Prior to benchtop testing, the microchannel was primed with deionized water for 10 minutes to remove air. The flow was applied using hydrostatic pressure, where the height difference between the reservoir and the device was changed incrementally from 15 cmH_2O to 0 cmH_2O in both forward and reverse directions (n=4 readings with one valve). A two-way stop-cock was added between the reservoir and device, to allow for control of flow through the valve. To calculate the flow rate, deionized water was allowed to flow through the valve for two seconds; the collected fluid was then weighed.

RESULTS AND DISCUSSION

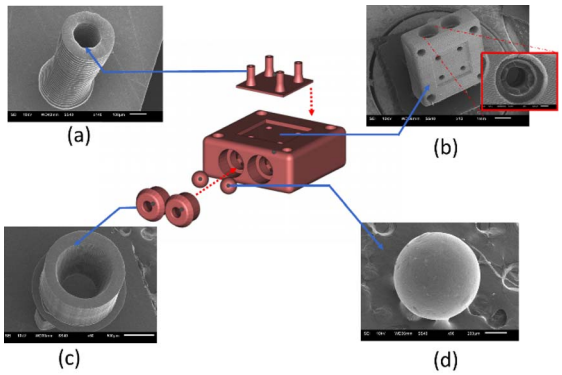

Fig. 3 *SEM images of the 3D printed objects (a) hollow microneedle (inner diameter 160 um, outer diameter 220 um, height 900 um) (b) the device with one end of a microchannel with larger cross-section (c) one end of a microchannel with smaller cross-section (d) a microbead of diameter 800 um*

Fig 3 shows scanning electron microscopy (SEM) images of 3D printed objects of the bead-based device. The dimensions are 5 mm length, 5 mm width, and 2 mm height. Dimensions were calculated based on the physiological flow rates of the CSF (0.25 mL/min bulk volumetric flow rate). Based on physiological conditions, change in pressure was estimated 420 Pa assuming the dynamic fluid viscosity was 0.6912×10^{-3} Pa/s. Based on these requirements the appropriate radius and lengths for the cylindrical needles were determined. Due to resolution requirements of the printer, the final measurements were

amended to a length of 900 um, an inner diameter of 160 um, and an outer diameter of 220 um.

The bead-based MAG device contains several components, (1) hollow microneedles to interface the dura (Fig 3a), (2) microchannel to allow for one way flow of the CSF (Fig 3b and Fig 3c), (3) and commercially available polymer microbeads with a diameter of 800 um. Assembly offered a closed system for operating pressure-flow testing. To 3D printing complex geometry, gravity was used to move the unexposed residue out of the microchannel. In the experiment, the embedded microchannels and bead-based valves were printed with a tiled angle (Ø), instead of starting from a flat surface. The tilted angle allows the unexposed resin inside the microchannels to be exposed during the layer-by-layer exposure of 3D printing. Without tilting (Ø=0), the square device with embedded circular microchannels (diameter 600 μm and length 5 mm) was would be completely, with the unexposed resin remaining inside the microchannels. The optimal angle (Ø) for 3D printing, which allowed for defect free printing of the microchannels, was experimentally deduced to be 50 degrees.

The Young's modulus of the resin used for microneedle fabrication was 1.02GPa, which may be too soft for the microneedles to penetrate through variations of dura, causing the needles to deform or become damaged. The biodegradable sugar aimed to resolve these issues. Sugar contains sweet, short-chain, soluble carbohydrates, and is rigid when solid. The system was designed such that the sugar would then dissolve within seconds of exposure to CSF. The literature has shown that the length and the geometry of sucrose coatings could be controlled by its viscosity and pulling speed [7]. When exposed to water, sucrose becomes fructose and glucose when being hydrolyzed. Sucrose was chosen due to its tunable viscosity with processing temperature. When the temperature was above decomposed temperature T_d (186C), sucrose was transformed into caramelized sucrose, where its viscosity and surface tension decreased with increasing temperature.

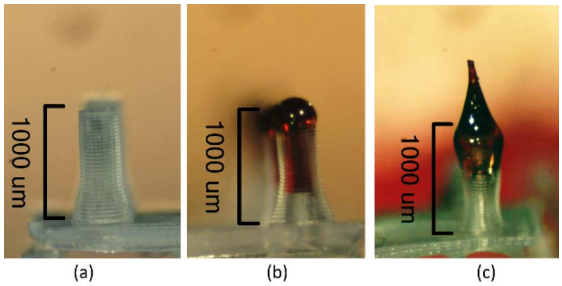

Fig. 4 *Modification of microneedles with biodegradable sugar coating. (a) Original, without manipulation, (b) following the first-step to fill the hollow channel, and (c) following the second-step to form the sharp tip.*

Fig 4 shows the result of modification of needle shapes with two-step coatings, where a sharp tip was able to form on the microneedles (in Fig 4c). It is critical that during the first coating the sucrose has low surface tension for the hollow needles to be immersed in caramelized sucrose. In the experiment, the temperature T_1 (275C) was found optimal for the task. The purpose of the second coating was to form a sharp tip to decrease resistance during penetration and to prevent structures from deformation. When the viscosity of caramelized sucrose was too high, the length of tip formation was long. On the other hand, the structure of sharp tips did not form when sucrose had very low viscosity. The temperature T_2 (175C) was found optimal to form sharp tips with proper length, which can be easily controlled by adjusting the pulling speed. In this case, 800 um/s was used to form a sharp cone-like tip with 500 um length on the top of microneedles.

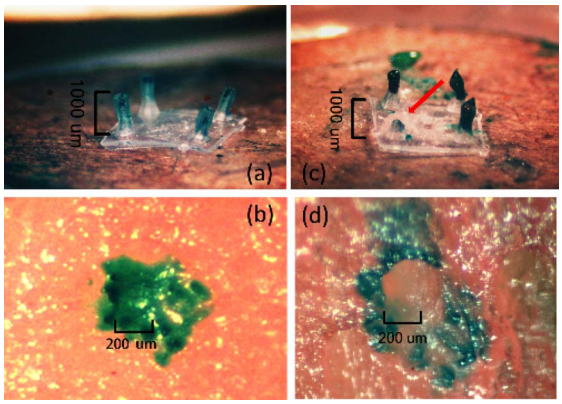

Fig. 5 *The penetration test of microneedles to porcine skin (a)(b) with the two-step sugar coating, and (c) d) without the two-step sugar coating.*

Fig 5 shows the preliminary tests to penetrate microneedles into porcine skin with (Fig. 5a) and without (Fig. 5c) the sugar coatings. As shown in Fig. 5b, without the sugar coating, the microneedles did not penetrate the animal skin, where they deformed, showing the flexibility of resin. In Fig. 5d, the microneedles with proper sugar

coatings could successfully penetrate skin. Future testing on explanted dura and in vivo will yield more physiologically relevant data for the microneedle optimization.

In Fig 6, the performance of the shunt valve is shown. The valve was able to regulate the pressure in the range 0-1500Pa with the flow rate up to 2 mL/min (significantly above the physiologic production or absorption rate of CSF). For reverse flow, the flow rate drops to zero when the reverse pressure was within 1500 Pa. The preliminary study shows the potential for a bead-based MAG to function within physiological relevant conditions (between -1000~1500 Pa). Importantly, the proposed device is passive and does not require any control circuit or power supply.

In conclusion, this paper investigates bead-based arachnoid granulations using 3D printing (stereolithography). The bead-based MAG device has been preliminarily tested, but additional samples are needed for appropriate statistical analyses of our methods. Future work will also be necessary to address the mechanical strength and degradation rate of the sugar coating to penetrate dura. Immediate testing will address compatibility with protein, cells of the CNS, and blood products in physiologic benchtop and in vitro flow tests. To date, there have not been studies on the long-term implantation of 3D printed prosthetic devices for CSF diversion; a research direction that we wish to explore in the future with an animal model.

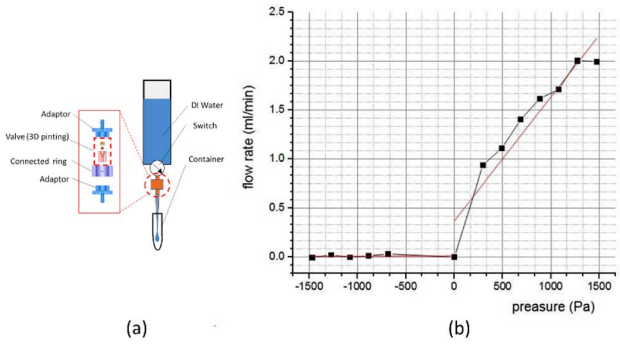

Fig 6 *The performance of the shunt valve (a) experimental set-up (b) the flow rate vs pressure*

REFERENCE

[1] F Kralick et al., Acta Neurochir Suppl 114: 239-42.

[2] Y Enchev and S Oi, Neurosurg Rev 31(3): 249-62.

[3] SA Lee et al., Conf Proc IEEE Med Biol Soc (2006) 1: 2494-7.

[4] S Johansson et al, Biomed Microdevices (2014) 16:529–536

[5] J Oh, et al, J. Microelectromech.Syst (2011) 20 (4) p811-818

[6] PJ Chen, et al, J. Microelectromech. Syst (2007) 16(2) p223-231

[7]Kwang Lee, et al, Biomaterials 33 (2012) 7309-7326